Int. J. Nanosci. Nanotechnol., Vol. 13, No. 2, June 2017, pp. 119-127

Surfactant Removal from Mesoporous Silica Shell of Core-Shell Magnetic Microspheres by Modified Supercritical CO_2

Z. Kheshti and Sh. Hassanajili*

Department of Chemical Engineering, School of Chemical and Petroleum Engineering, Shiraz University, Shiraz 7193616511, Iran

(*) Corresponding author: ajili@shirazu.ac.ir
(Received: 22 October 2015 and Accepted: 07 August 2016)

Abstract

In this paper, a kind of core–shell magnetic mesoporous microspheres of Fe_3O_4@SiO_2@meso-SiO_2 with high surface area was prepared, where magnetic Fe_3O_4 nanospheres were used as the inner core, tetraethyl orthosilicate (TEOS) as silica source, and cetyltrimethylamonium bromide (CTAB) as pore forming agent. Methanol-enhanced supercritical CO_2 extraction has been attempted on structurally order mesoporous shell to remove the cationic template of CTAB and the effects of operating conditions i.e. pressure and temperature on the extraction efficiency were investigated. The influence of the methanol-enhanced supercritical CO_2 on the structural properties of magnetic mesoporous silica nanocomposites was examined in detail by means of FE-SEM, FTIR, XRD, N_2 adsorption/desorption and VSM. The obtained results reflected that the methanol-enhanced supercritical CO_2 extraction had well preserved the structural stability of Fe_3O_4@SiO_2@meso-SiO_2 with high surface area ca. 569 m^2/g. The strong magnetization value (60 emu/ g) of the core–shell particles suggests their suitability for magnetic separation in a short time.

Keywords: *Supercritical fluid extraction, Magnetic nanoparticle, Core-shell structure, Mesoporous silica, Modifier, Template removal.*

1. INRODUCTION

Core–shell components have been studied extensively over the last decade due to their potential applications [1-4]. Different from single-component that can only supply people with specific property; the core–shell components can integrate multiple advantages into one system for specific application [5, 6]. Among the core–shell structured composites, the composites with magnetic core and functionalized shell have attracted particular interest, mainly due to their potential applications in catalysis, drug delivery, adsorption, chromatography, and chemical or biologic sensors [7-13]. The inner core is composed of Fe_3O_4 nanospheres with magnetically responsive core makes it easy to recycle, the outer shell is nonporous silica shell which protect the magnetite from etching in harsh application occasions. In addition, the mesoporous silica shell is created on the structure by combination of CTAB- based self-assembly and sol-gel processing, in order to achieve higher adsorptive surface area which makes their further functionalization more convenient [8, 14, 15]. Several strategies for removing organic templates have been documented, including calcinations at high temperature, solvent extraction and supercritical fluid CO_2 extraction (SCF-CO_2) [16-23].

Calcination is frequently used to burn off organic templates at high temperatures. Although organic templates can completely be removed, but it is a time Therefore, a polar modifier like CH_3OH has been usually added to $SCCO_2$ for high effectiveness extraction of such compounds. The addition of a small amount of a polar organic modifier could significantly enhance the solvating power

of SCF-CO_2 to targeted organic templates [27-29, 34, 35]. In this paper, we have attempted to prepare a kind of novel Fe_3O_4 @SiO_2@*meso*-SiO_2 microspheres that was directly introduced into the system by syringe pump with flow rate by a liquid metering pump along with CO_2 flow. An optimal ratio of CH_3OH/CO_2 (0.1/1.0 ml/min) as feed and the extraction time of 3 h which were found out from other studies [26, 32, 33], used in this work. Then, the system was slowly depressurized at the experimental temperature. The surfactant (CTAB) was dissolved into the SCF-CO_2 in order to extract the template without any damaging effects on the structure of core-shell. The properties of the obtained materials were characterized by transmission electron microscopy (TEM), scanning electron microscopy (SEM), N_2 adsorption-desorption and X-ray powder diffraction. The synthesized sample had a higher pore volume and surface area than those of the microspheres reported in the latest literatures [8, 17, 25, 36-38]

2. EXPERIMENTAL

2.1. Materials

Ferric chloride hexahydrate ($FeCl_3.6H_2O$), ferrous choliride teterahydrate ($FeCl_2.4H_2O$), tetraethyl orthosilicate (TEOS), NH_4OH (28%), cetyltrimethylammonium bromide (CTAB), toluene and absolute alcohol (EtOH) were purchased from Merck Co., Germany.

2.2. Methods

2.2.1. Synthesis of Magnetic Nanoparticles (MNPs)

Fe_3O_4 magnetic nanoparticles (MNPs) were synthesized by chemical co-precipitation method [39]. Briefly, $FeCl_3.6H_2O$ and $FeCl_2.4H_2O$ (molar ratio, 1:2) were dissolved in deionized water. At 80 ^oC about 20 ml of NH_4OH solution was added under vigorous stirring in the presence of nitrogen atmosphere for 20 min. Afterwards, the black precipitate Fe_3O_4 was collected, washed with ethanol and deionized water and dried at 60 ^oC under vacuum overnight.

2.2.2. Synthesis of Fe_3O_4@SiO_2 Nanoparticles

Silica was coated on MNPs, by dispersing the MNPs in a flask containing 80 ml of ethanol and 20 ml of deionized water followed by sonication. The pH was maintained at 10 throughout the process by addition of ammonium hydroxide. During sonication, 0.4 ml of TEOS was added dropwise and after stirring for 8 h in the presence of nitrogen gas, the products were collected and washed with ethanol and deionized water, and dried under vacuum at 80 ^oC for 4 h.

2.2.3. Synthesis of Fe_3O_4@SiO_2@*meso*-SiO_2 Microspheres

The core-shell magnetic mesoporous Fe_3O_4@SiO_2@*meso*-SiO_2 microspheres with large mesopore size were prepared by the methodology described in ref [15] with some modifications. As-made Fe_3O_4@SiO_2 nanoparticles were dispersed in a mixed solution containing ethanol (30ml), deionized water (40 ml), and concentrated ammonia solution (1.5ml), and the solution was ultrasonicated for 45 min. then, CTAB (0.3 gr) was added into solution and ultrasonicated for another 45 min. subsequently, 0.5 ml of TEOS was added dropwise to the solution, after mechanical agitation for 10 h, the obtained particles were separated, washed with deionized water and dried under vacuum.

2.2.4. Template Removal

The methanol enhanced-SCF-CO_2 extraction, used for template CTAB removal from as-synthesized adsorbent, according to the method described in the literature [28, 30, 31, 34]. The experimental procedure may be briefed as follows. An as-synthesized Fe_3O_4@SiO_2@*meso*-SiO_2 microsphere was

packed in the extraction vessel. The liquid CO_2 were introduced into vessel (with flow rate 1 ml/min) by high pressure metering pump for 3 h. Methanol as polar modifier CO_2/modifier in the extraction vessel and removed from structure. A schematic of the experimental setup is shown in Fig.1. To study the influence of operating conditions, different temperatures between 70-90^oC and pressures in the range 150 to 210 bar were chosen and the amount of template in the samples were determined by thermogravimetric analysis (TGA). The extraction efficiency was estimated by measuring the amount of template remaining on the both as-synthesized and methanol-enhanced-SCF-CO_2 processed samples by comparing their weight losses.

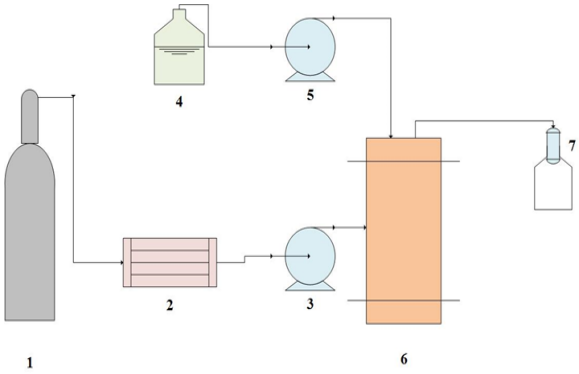

Figure 1*. A schematic diagram for the experimental apparatus of modifier supercritical CO_2 extraction: (1) CO_2 cylinder, (2) condenser, (3) pump, (4) methanol reservoir (5) pump, (6) extraction vessel, (7) collection tube.*

3. CHARACTERIZATION

Fourier transform-infrared (FT-IR) spectra were recorded on a Perkin-Elmer spectrophotometer using KBr pellet technique. Structure and morphology of the products were characterized by field emission scanning electron microscopy (FE-SEM, Hitachi1460, Japan). Nitrogen adsorption and desorption isotherm were measured at a liquid nitrogen temperature (77K) using a PHS-1020 (PHS, CHINA) analyzer. The specific surface area was calculated by the Brunaure-Emmett-Teller (BET) method. Pore volume and porosity were determined using Barret-Joyner-Halenda (BJH) model, respectively. X-ray diffraction (XRD) measurements were carried out with Burker AXS D8-advance X-ray diffractometer with CuK_α radiation. Thermogravimetric analysis (TGA) data were determined on Mettle-Toledo thermal instrument from 20 to 750 ^oC with a heating rate of 10 ^oC/min under nitrogen flow. Particle size analyzer was utilized using PSA (JAPA Horiba LB 550).

4. RESULTS AND DISCUSSION

4.1. Effect of Temperature and Pressure

The experimental conditions for performing methanol-enhanced-SCF-CO_2 of CTAB were optimized with as-prepared Fe_3O_4@SiO_2@*meso*-SiO_2 microspheres regard to extraction temperature and pressure. Fig. 2a shows the TGA results of the SCF-processed samples with respective pressure 150, 180 and 210 bar (T: 80^oC, CH_3OH/CO_2 ratio: 0.1/1.0 ml/min, t: 3h) along with the as-synthesized sample. The increase in extraction efficiency can be attributed to the increase in density and solvating ability of the supercritical fluid with increasing pressure. Therefore, the optimized pressure (180 bar) for higher extraction of templates (78%) is obtained.
Fig. 2b shows the TGA results of the SCF-processed samples with respective temperature 70, 80 and 90 °C (P: 180 bar, CH_3OH/CO_2 ratio: 0.1/1.0 ml/min, t: 3h) along with the as-synthesized sample. As seen, at 180 bar the increase of temperature from 70 to 80 ^oC results in the increase of the extraction efficiency (78%), whereas the increase of temperature above 80 ^oC leads to the decrease of the extraction efficiency approximately. This is may be related to the cationic nature of CTAB which leads to its strong attachment to the matrix pore surface via electrostatic interaction [40]. Thus to effectively remove the template CTAB, the matrix/template interactions must be overcome through thermal energy supplied during extraction by selective interaction of the CO_2-modifier molecules with the

matrix-template complex. By increasing the temperature above 80°C, the extraction efficiency decreased due to decreased the solubility of template in the supercritical fluid. Similar observations have been reported in several researches [41-43]. From the above results, the optimum temperature and pressure for effectively extraction of CTAB from the structure with CO_2-methanol mixture are 80 °C and 180 bar, respectively. The extraction efficiencies obtained at different pressures and temperatures are shown in Table 1. In the following parts, the structural properties of resultant optimized samples were characterized in detail.

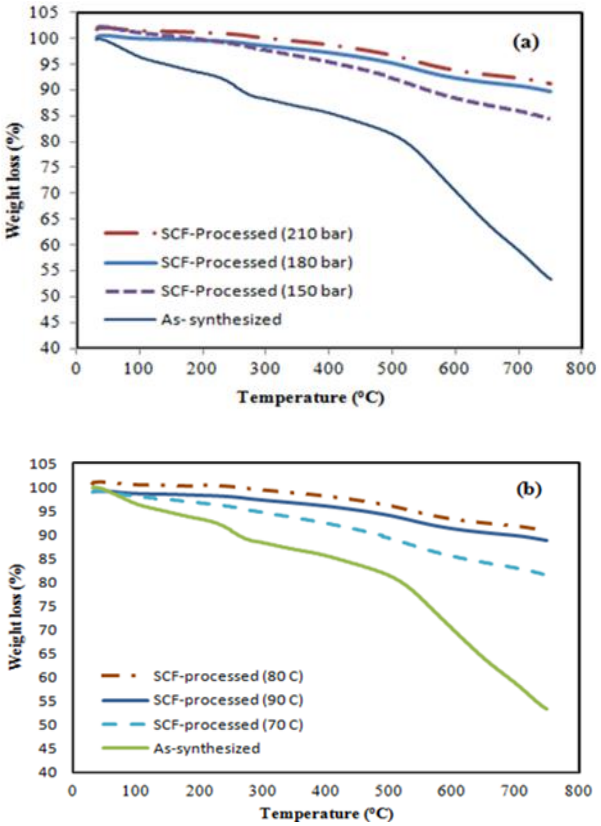

***Figure 2**. TGA curves of as-synthesized Fe_3O_4@SiO_2@ meso-SiO_2 sample powders and SCF- processed samples with (a) different pressures (T: 80°C, CH_3OH/CO_2 ratio: 0.1/1.0 ml/min, t: 3h) and (b) different temperatures (P: 180 bar, CH_3OH/CO_2 ratio: 0.1/1.0 ml/min, t: 3h).*

***Table 1**. SCF extraction efficiency obtained at different pressures and temperatures.*

Condition	Extraction Efficiency (%)
P=150 bar & T=80 °C	68
P=180 bar & T=80 °C	78
P=210 bar & T=80 °C	79
T=70 °C & P= 180 bar	62
T=80 °C & P= 180 bar	78
T=90 °C & P= 180 bar	75

4.2. Characterization of the Multi-functional Mesoporous Microspheres

4.2.1 Morphological Study

The particle size and morphology of Fe_3O_4, Fe_3O_4@SiO_2 and Fe_3O_4@SiO_2@*meso*-SiO_2 were analyzed by FE-SEM micrographs and PSA images. The mean diameter of Fe_3O_4 nanoparticles is 7 nm with a spherical shape as shown in Fig. 3a. Moreover, the Fe_3O_4 nanoparticles are composed of many smaller nanoparticles with rough surface. After the sol-gel process, the Fe_3O_4@SiO_2 particles had an overall mean diameter of ~ 18 nm (Fig. 3b) and the smooth surfaces of the obtained Fe_3O_4@SiO_2nanoparticles indicate that the SiO_2 layer was coated successfully onto the Fe_3O_4 nanoparticles. In Fig 3.c we can observe that Fe_3O_4@SiO_2@*meso*-SiO_2 microspheres still exhibit a core-shell structure with about 370 nm diameter.

4.2.2. Fourier Transform Infrared Spectroscopy Analysis

The FTIR spectra of Fe_3O_4 and Fe_3O_4@SiO_2@*meso*-SiO_2 are shown in Fig.4. The typical absorption peak for Fe_3O_4 at 594 cm^{-1} is an indication of the presence of Fe-O [44-46]. The weak and broad band around 3440 cm^{-1} is the typical O-H stretching vibration modes of adsorbed water [46, 47].

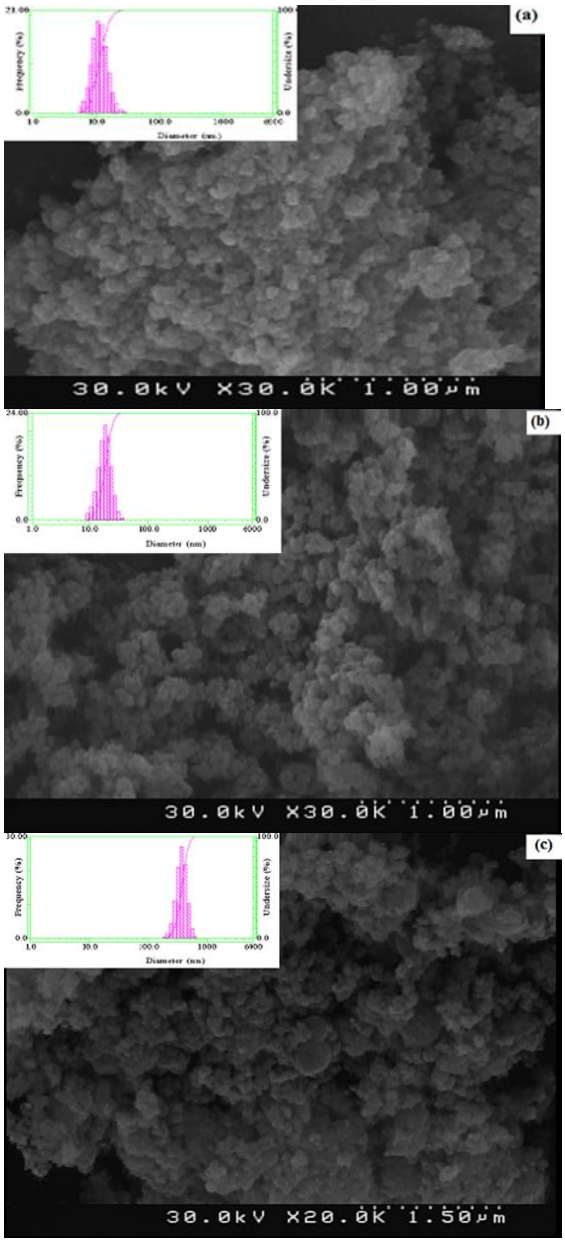

***Figure 3**. FE-SEM images and PSA results of (a) Fe_3O_4, (b) Fe_3O_4@SiO_2 and (c) Fe_3O_4@SiO_2@meso-SiO_2.*

The adsorption peaks at 1056 and 801 cm^{-1} result from asymmetric and symmetric vibration of Si-O-Si band in oxygen-silica tetrahedron, which confirms that the formation of silica layer on the surface of magnetic nanoparticles [17, 47-49].

4.2.3. N_2 Adsorption-Desorption Isotherm

The N_2 adsorption-desorption isotherm of Fe_3O_4@SiO_2@*meso*-SiO_2 in Fig.5

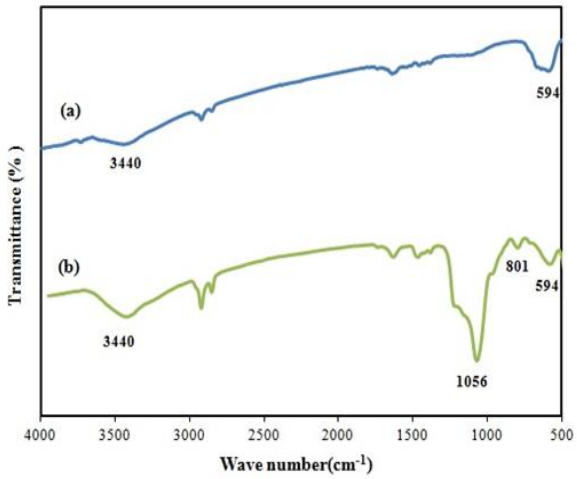

***Figure 4**. FTIR spectra of (a) Fe_3O_4 and (b) Fe_3O_4@SiO_2@meso-SiO_2.*

shows IV-type curve with H_1-hysteresis loop, which is usually attributed to the presence of well-uniform mesopores [25, 36]. The average mesopore size of these sample is 2.5 nm. The BET surface area and pore volume are 568.729 m^2 g^{-1} and 0.55 cm^3 g $^{-1}$, respectively. As shown in Table 2 the obtained surface area and pore volume are higher than those samples which have been made by calcination or solvent extraction methods in previous studies. Therefore this large pore volume (size) can be very beneficial for the surface treatment to provide the opportunity for selective adsorption.

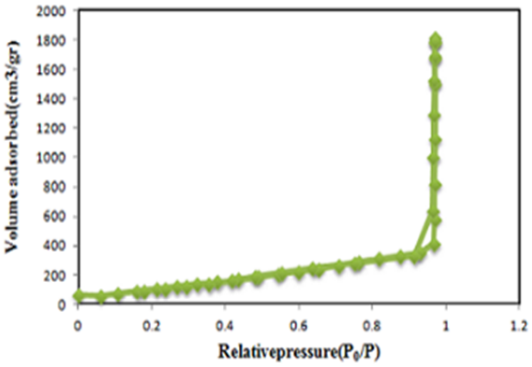

***Figure 5.** Nitrogen adsorption-desorption of Fe_3O_4@SiO_2@meso-SiO_2.*

4.2.4. XRD Analysis

The XRD patterns of the samples, including Fe_3O_4, Fe_3O_4@SiO_2 and

***Table 2**. Comparison of pore features for Fe_3O_4@SiO_2@meso-SiO_2 microsphere in references.*

Pore volume (cm^3/g)	BET surface area (m^2/g)	Reference
0.41	378	[8]
0.28	274	[38]
0.18	403	[16]
-	359	[37]
0.24	202	[17]
0.21	293	[26]
0.55	569	This work

Fe_3O_4@SiO_2@*meso*-SiO_2 are presented in Fig.6. Five characteristics peaks occurred at 2θ of 30.25 °, 35.64 °, 43.26 °, 53.66 °, 57.18 ° and 62.78 ° could be assigned to 220, 311, 400, 422, 511 and 440 for Fe_3O_4 were similar to the other samples which indicates that the crystalline structure of Fe_3O_4 were pure and there was no phase change in MNPs before and after surface coating and modification [50].

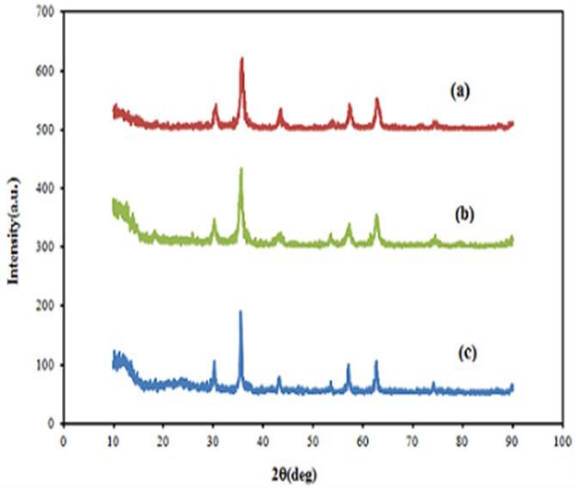

***Figure 6.** XRD patterns of (a) Fe_3O_4, (b) Fe_3O_4@SiO_2 and (c) Fe_3O_4@SiO_2@meso-SiO_2.*

4.2.5. Vibrating Sample Magnetometer (VSM)

The magnetic hysteresis loops of Fe_3O_4 and Fe_3O_4@SiO_2@*meso*-SiO_2 are shown in Fig. 8 at room temperature. The saturation magnetizations of Fe_3O_4 and Fe_3O_4@SiO_2@*meso*-SiO_2 were 82 and 60 emu/g, which suggested that magnetic mesoporous silica show excellent magnetic property and they can be rapidly separated from solution with permanent hand-held magnets within a 20 second.

***Figure 7**. Separation of the Fe_3O_4@SiO_2@meso-SiO_2 particles by a magnet during 20 s.*

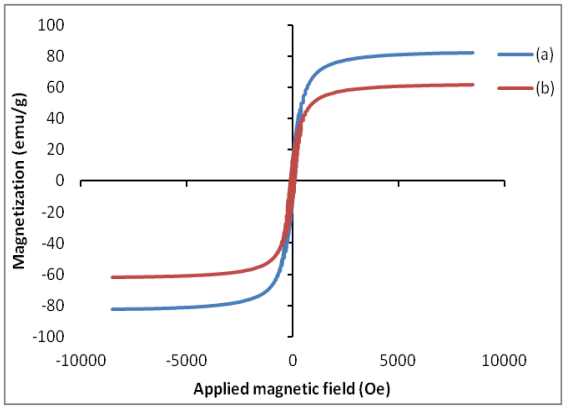

***Figure 8**. VSM curves of (a) Fe_3O_4 and (b) Fe_3O_4@SiO_2@meso-SiO_2*

5. CONCLUSION

In this study, we prepared a novel Fe_3O_4@SiO_2@*meso*-SiO_2 microspheres with high BET surface area and superparamagnetic properties. The application of supercritical CO_2-methanol mixture extraction has been examined for synthesized magnetic mesoporous powders with cetyltrimethylamonium bromide as the organic template. The effect of pressure and temperature on the extraction

efficiency of CTAB is discussed in detail. The results indicated that over 75% of the organic template can be successfully recovered within 3 h under optimal conditions of 180 bar and 80 ^{o}C. Besides, the characterization studies depicted that the morphology and structure of Fe_3O_4 did not change significantly due to the coating, template extraction and modification stages.

6. ACKNOWLEDGEMENT

Dr. Feridun Esmaeilzadeh, department of Chemical Engineering, Shiraz University, is greatly acknowledged for his technical support for our experiments. The authors are also grateful to Dr. Ghodratollah Absalan, department of chemistry, collage of science, Shiraz University for his kind assistance**.**

REFERENCES

1. Nikje, M. M. A., Sarchami, L.,Rahmani, L. (2015). "Fabrication of 2-Chloropyridine-Functionalized Fe3O4/Amino-Silane Core–Shell Nanoparticles", *International Journal of Nanoscience and Nanotechnology*, 11: 39-44.
2. Teng, X., Black, D., Watkins, N. J., Gao, Y., Yang, H. (2003). "Platinum-Maghemite Core−Shell Nanoparticles Using a Sequential Synthesis", *Nano Letters*, 3: 261-264.
3. Jiang-Ying Li, S. X., Pan, J., Qian, Y. (May 12, 2010). "Hydrothermal Synthesis and Electrochemical Properties of Urchin-Like Core−Shell Copper Oxide Nanostructures", *Physics and Chemistry*, 114 (21): 9645–9650.
4. Zhu, C.-L., Zhang, M.-L., Qiao, Y.-J., Xiao, G., Zhang, F., Chen, Y.-J. (2010). "Fe3O4/TiO2 Core/Shell Nanotubes: Synthesis and Magnetic and Electromagnetic Wave Absorption Characteristics", *The Journal of Physical Chemistry C*, 114: 16229-16235.
5. Hu, J. Q., Zhan Y. B., J. H., Golberg, D. (2004). "Si*/*ZnS and Si*/*ZnSe core/shell nanocrystal structures", *Applied Physics Letters*, 85: 3593.
6. Cao, J., Hong, J.-Z. S., J., Li, H.-Y., Chen, H.-Z., Wang, M. (January, 2004). "Carbon Nanotube/CdS Core–Shell Nanowires Prepared by a Simple Room-Temperature Chemical Reduction Method", *ADVANCED MATERIALS*, 16: 84–87.
7. Jennifer L. Lyon, D. A. F., Stone, M. B., Schiffer, P., Williams, . E. (March 20, 2004). "Synthesis of Fe Oxide Core/Au Shell Nanoparticles by Iterative Hydroxylamine Seeding", *Nano Letters*, 4: 719–723.
8. Yang, P., Quan, Z., Hou, Z., Li, C., Kang, X., Cheng, Z., Lin, J. (2009). "A magnetic, luminescent and mesoporous core–shell structured composite material as drug carrier", *Biomaterials*, 30: 4786-4795.
9. Zhang, M., Wu, Y., Feng, X., He, X., Chen, L., Zhang, Y. (2010). "Fabrication of mesoporous silica-coated CNTs and application in size-selective protein separation", *Journal of Materials Chemistry*, 20: 5835-5842.
10. Won, Y.-H., Aboagye, D., Jang, H. S., Jitianu, A., Stanciu, L. A. (2010). "Core/shell nanoparticles as hybrid platforms for the fabrication of a hydrogen peroxide biosensor", *Journal of Materials Chemistry*, 20: 5030-5034.
11. Li, Y., Wu, J., Qi, D., Xu, X., Deng, C., Yang, P., Zhang, X. (2008). "Novel approach for the synthesis of Fe3O4@TiO2 core-shell microspheres and their application to the highly specific capture of phosphopeptides for MALDI-TOF MS analysis", *Chemical Communications*: 564-566.
12. Moradian, M., Moradian, M., Boroumand, Z. (2013). "A New and Efficient Method for the Adsorption and Separation of Arsenic Metal Ion from Mining Waste Waters of Zarshouran Gold Mine by Magnetic Solid-Phase Extraction with Modified Magnetic Nanoparticles", *International Journal of Nanoscience and Nanotechnology*, 9: 121-126.
13. Khayat Sarkar, Z., Khayat Sarkar, F. (2013). "Selective Removal of Lead (II) Ion from Wastewater Using Superparamagnetic Monodispersed Iron Oxide (Fe3O4) Nanoparticles as a Effective Adsorbent", *International Journal of Nanoscience and Nanotechnology*, 9: 109-114.
14. Xu, Z., Li, C., Kang, X., Yang, D., Yang, P., Hou, Z., Lin, J. (2010). "Synthesis of a Multifunctional Nanocomposite with Magnetic, Mesoporous, and Near-IR Absorption Properties", *The Journal of Physical Chemistry C*, 114: 16343-16350.
15. Deng, Y., Qi, D., Deng, C., Zhang, X., Zhao, D. (2008). "Superparamagnetic High-Magnetization Microspheres with an Fe3O4@SiO2 Core and Perpendicularly Aligned Mesoporous SiO2 Shell for Removal of Microcystins", *Journal of the American Chemical Society*, 130: 28-29.
16. Zhao, L., Chi, Y., Yuan, Q., Li, N., Yan, W., Li, X. (2013). "Phosphotungstic acid anchored to amino–functionalized core–shell magnetic mesoporous silica microspheres: A magnetically recoverable nanocomposite with enhanced photocatalytic activity", *Journal of Colloid and Interface Science*, 390: 70-77.

17. Li, W., Zhang, B., Li, X., Zhang, H., Zhang, Q. (2013). "Preparation and characterization of novel immobilized Fe3O4@SiO2@mSiO2–Pd(0) catalyst with large pore-size mesoporous for Suzuki coupling reaction", *Applied Catalysis A: General*, 459: 65-72.
18. Yuan, Q., Li, N., Chi, Y., Geng, W., Yan, W., Zhao, Y., Li, X., Dong, B. (2013). "Effect of large pore size of multifunctional mesoporous microsphere on removal of heavy metal ions", *Journal of Hazardous Materials*, 254–255: 157-165.
19. Wu, S., Wang, H., Tao, S., Wang, C., Zhang, L., Liu, Z., Meng, C. (2011). "Magnetic loading of tyrosinase-Fe3O4/mesoporous silica core/shell microspheres for high sensitive electrochemical biosensing", *Analytica Chimica Acta*, 686: 81-86.
20. Liu, H., Ji, S., Yang, H., Zhang, H., Tang, M. (2014). "Ultrasonic-assisted ultra-rapid synthesis of monodisperse meso-SiO2@Fe3O4 microspheres with enhanced mesoporous structure", *Ultrasonics Sonochemistry*, 21: 505-512.
21. Tang, Y., Liang, S., Wang, J., Yu, S.,Wang, Y. (2013). "Amino-functionalized core-shell magnetic mesoporous composite microspheres for Pb(II) and Cd(II) removal", *Journal of Environmental Sciences*, 25: 830-837.
22. Min, B. U.,Wenzhong, M. (2013). "Study on core–shell–shell structured nanoparticles with magnetic and luminescent features: Construction, characterization and oxygen-sensing behavior", *Journal of Luminescence*, 141: 80-86.
23. Ryczkowski, J., Goworek, J., Gac, W., Pasieczna, S., Borowiecki, T. (2005). "Temperature removal of templating agent from MCM-41 silica materials", *Thermochimica Acta*, 434: 2-8.
24. Tanev, P. T., Pinnavaia, T. J. (1996). "Mesoporous Silica Molecular Sieves Prepared by Ionic and Neutral Surfactant Templating: A Comparison of Physical Properties", *Chemistry of Materials*, 8: 2068-2079.
25. Lian, L., Cao, X., Wu, Y., Lou, D., Han, D. (2013). "Synthesis of organo-functionalized magnetic microspheres and application for anionic dye removal", *Journal of the Taiwan Institute of Chemical Engineers*, 44: 67-73.
26. Ibrahim, A. S. S., Al-Salamah, A. A., El-Toni, A. M., El-Tayeb, M. A., Elbadawi, Y. B. (2014). "Cyclodextrin glucanotransferase immobilization onto functionalized magnetic double mesoporous core–shell silica nanospheres", *Electronic Journal of Biotechnology*, 17: 55-64.
27. Huang, Z., Luan, D. Y., Shen, S. C., Hidajat, K.,Kawi, S. (2005). "Supercritical fluid extraction of the organic template from synthesized porous materials: effect of pore size", *The Journal of Supercritical Fluids*, 35: 40-48.
28. Kawi, S., Lai, M. W. (2002). "Supercritical fluid extraction of surfactant from Si-MCM-41", *AIChE Journal*, 48: 1572-1580.
29. Kawi, S., Goh, A. H., "Supercritical Fluid Extraction of Amine Surfactant in Hexagonal Mesoporous Silica (HMS)," in *Studies in Surface Science and Catalysis*. vol. Volume 129, S. Abdelhamid., J. Mietek, Eds., ed: Elsevier, 2000, pp. 131-138.
30. Huang, Z., Xu, L., Li, J.-H., Kawi, S., Goh, A. H. (2011). "Organic template removal from hexagonal mesoporous silica by means of methanol-enhanced CO2 extraction: Effect of temperature, pressure and flow rate", *Separation and Purification Technology*, 77: 112-119.
31. Huang, Z., Xu, L., Li, J.-H. (2011). "Amine extraction from hexagonal mesoporous silica materials by means of methanol-enhanced supercritical CO2: Experimental and modeling", *Chemical Engineering Journal*, 166: 461-467.
32. Fung, Y. S., Long, Y. H. (2001). "Determination of phenols in soil by supercritical fluid extraction–capillary electrochromatography", *Journal of Chromatography A*, 907: 301-311.
33. Chatterjee, M., Hayashi, H., Saito, N. (2003). "Role and effect of supercritical fluid extraction of template on the Ti(IV) active sites of Ti-MCM-41", *Microporous and Mesoporous Materials*, 57: 143-155.
34. Huang, Z., Huang, L., Shen, S. C., Poh, C. C., Hidajat, K., Kawi, S., Ng, S. C. (2005). "High quality mesoporous materials prepared by supercritical fluid extraction: effect of curing treatment on their structural stability", *Microporous and Mesoporous Materials*, 80: 157-163.
35. Van Grieken, R., Calleja, G., Stucky, G. D., Melero, J. A., García, R. A., Iglesias, J. (2003). "Supercritical Fluid Extraction of a Nonionic Surfactant Template from SBA-15 Materials and Consequences on the Porous Structure", *Langmuir*, 19: 3966-3973.
36. Liu, Z., Yang, H., Zhang, H., Huang, C., Li, L. (2012). "Oil-field wastewater purification by magnetic separation technique using a novel magnetic nanoparticle", *Cryogenics*, 52: 699-703.
37. Aboufazeli, F., Lotfi Zadeh Zhad, H. R., Sadeghi, O., Karimi, M., Najafi, E. (2013). "Novel ion imprinted polymer magnetic mesoporous silica nano-particles for selective separation and determination of lead ions in food samples", *Food Chemistry*, 141: 3459-3465.

38. Li, Z., Huang, D., Fu, C., Wei, B., Yu, W., Deng, C., Zhang, X. (2011). "Preparation of magnetic core mesoporous shell microspheres with C18-modified interior pore-walls for fast extraction and analysis of phthalates in water samples", *Journal of Chromatography A,* 1218: 6232-6239.
39. Zhao, X., Wang, J., Wu, F., Wang, T., Cai, Y., Shi, Y., Jiang, G. (2010). "Removal of fluoride from aqueous media by Fe3O4@Al(OH)3 magnetic nanoparticles", *Journal of Hazardous Materials,* 173: 102-109.
40. Huang, L., Kawi, S., Poh, C., Hidajat, K., Ng, S. C. (2005). "Extraction of cationic surfactant templates from mesoporous materials by CH3OH-modified CO2 supercritical fluid", *Talanta,* 66: 943-951.
41. Passos, C. P., Silva, R. M., Da Silva, F. A., Coimbra, M. A., Silva, C. M. (2010). "Supercritical fluid extraction of grape seed (Vitis vinifera L.) oil. Effect of the operating conditions upon oil composition and antioxidant capacity", *Chemical Engineering Journal,* 160: 634-640.
42. Macías-Sánchez, M. D., Serrano, C. M., Rodríguez, M. R.,Martínez de la Ossa, E. (2009). "Kinetics of the supercritical fluid extraction of carotenoids from microalgae with CO2 and ethanol as cosolvent", *Chemical Engineering Journal,* 150: 104-113.
43. Salgın, U., Döker, O., Çalımlı, A. (2006). "Extraction of sunflower oil with supercritical CO2: Experiments and modeling", *The Journal of Supercritical Fluids,* 38: 326-331.
44. Fan, F.-L., Qin, Z., Bai, J., Rong, W.-D., Fan, F.-Y., Tian, W., Wu, X.-L., Wang, Y., Zhao, L. (2012). "Rapid removal of uranium from aqueous solutions using magnetic Fe3O4@SiO2 composite particles", *Journal of Environmental Radioactivity,* 106: 40-46.
45. Hu, H., Wang, Z., Pan, L. (2010). "Synthesis of monodisperse Fe3O4@silica core–shell microspheres and their application for removal of heavy metal ions from water", *Journal of Alloys and Compounds,* 492: 656-661.
46. Lan, S., Wu, X., Li, L., Li, M., Guo, F., Gan, S. (2013). "Synthesis and characterization of hyaluronic acid-supported magnetic microspheres for copper ions removal", *Colloids and Surfaces A: Physicochemical and Engineering Aspects,* 425: 42-50.
47. Khosroshahi, M. E., Ghazanfari, L. (2012). "Synthesis and functionalization of SiO2 coated Fe3O4 nanoparticles with amine groups based on self-assembly", *Materials Science and Engineering: C,* 32: 1043-1049.
48. Xu, Y., Zhou, Y., Ma, W., Wang, S., Li, S. (2013). "Highly sensitive and selective OFF-ON fluorescent sensor based on functionalized Fe3O4@SiO2 nanoparticles for detection of Zn2+ in acetonitrile media", *Applied Surface Science,* 276: 705-710.
49. Zhang, J., Zhai, S., Li, S., Xiao, Z., Song, Y., An, Q., Tian, G. (2013). "Pb(II) removal of Fe3O4@SiO2–NH2 core–shell nanomaterials prepared via a controllable sol–gel process", *Chemical Engineering Journal,* 215–216: 461-471.
50. Ren, Y., Abbood, H. A., He, F., Peng, H., Huang, K. (2013). "Magnetic EDTA-modified chitosan/SiO2/Fe3O4 adsorbent: Preparation, characterization, and application in heavy metal adsorption", *Chemical Engineering Journal,* 226: 300-311.